



Three-Dimensional Neutronics Analysis for the ITER Divertor Cassette Design Options

M.E. Sawan, R.T. Santoro

June 1998

UWFDM-1077

Presented at the 13th Topical Meeting on the Technology of Fusion Energy,
June 7-11, 1998, Nashville TN

FUSION TECHNOLOGY INSTITUTE

UNIVERSITY OF WISCONSIN

MADISON WISCONSIN

THREE-DIMENSIONAL NEUTRONICS ANALYSIS FOR THE ITER DIVERTOR CASSETTE DESIGN OPTIONS

M.E. Sawan
University of Wisconsin-Madison
Fusion Technology Institute
1500 Engineering Drive
Madison, WI 53706 USA (608) 263-5093

R.T. Santoro
ITER JCT, Garching Co-Center
Boltzmannstrasse 2
85748 Garching
GERMANY

ABSTRACT

Three-dimensional neutronics calculations have been performed for the ITER divertor cassette design options to determine the nuclear parameters in the cassettes and assess the impact of streaming on vacuum vessel and toroidal field (TF) coil damage. The local nuclear parameters in the components of the reference cassette design are similar or lower than those in the cassette design option with wings. The total nuclear heating in the 60 divertor cassettes is 102 MW for both designs. Helium production levels in the vacuum vessel in the divertor region allow for rewelding. The TF coils are well protected from radiation streaming into the divertor ports.

I. INTRODUCTION

The International Thermonuclear Experimental Reactor (ITER) employs a modular single null divertor at the bottom of the machine¹. The divertor is segmented into 60 cassettes mounted on toroidal rails welded to the lower section of the vacuum vessel (VV). Each cassette is 5 m long, 2 m high and 0.5 - 1.0 m wide, and weighs about 25 tonnes. A dome is positioned immediately below the plasma X-point. The cassette configuration accommodates divertor channels for the inner and outer legs of the separatrix. Both channels are pumped in the private region beneath the dome through pumping ducts in the cassette body. Plasma facing components (PFC) that can handle the high surface heat flux are attached to the dome and surfaces surrounding the divertor channels.

The divertor cassette design has undergone several changes to improve its performance. In one of these design options, each divertor channel is surrounded by a vertical target, an assembly of wings and a gas box liner² as shown in Fig. 1. Several design options were considered for the dome, liner, dump target, and pumping ducts. The reference cassette design considered in the ITER final design includes an extended dome, elimination of the wings, and use of a thick liner in front of the pumping duct as shown in Fig. 2. In addition, the size of the pumping duct is different from that in the previous design option.

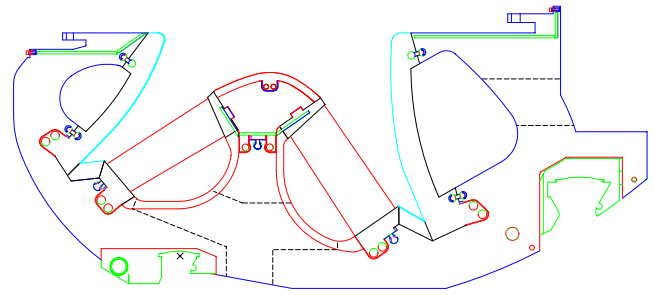


Fig. 1. The divertor cassette design option with gas boxes and wings under the dome.

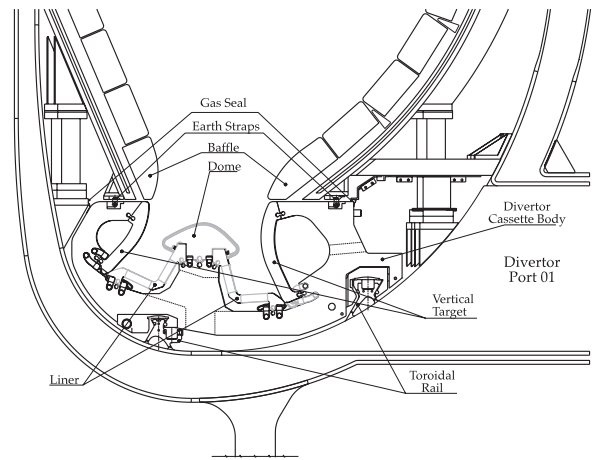


Fig. 2. Cross section of the reference divertor cassette.

Knowledge of nuclear heating and radiation damage levels in the different components of the divertor cassette is essential for proper design analysis. 20 large divertor ports are utilized for assembly and disassembly of the divertor cassettes and for vacuum pumping. Radiation streaming into these ports can produce excessive heating and damage in the TF coils in the divertor region. Reducing nuclear heating and radiation damage in the TF coils to acceptable levels is an important shielding issue. Radiation damage to parts of the VV in the divertor region need to be quantified to assess the feasibility of rewelding.

Three-dimensional (3-D) neutronics calculations have been performed for the ITER divertor to determine the nuclear parameters in the cassettes and assess the impact of streaming on VV and TF coil damage. The results will be presented for the cassette design option in which gas boxes are utilized with semi-transparent wings under the dome and for the current reference design taking into account the changes in geometry and material composition.

II. CALCULATIONAL MODEL

3-D neutron-gamma transport calculations have been performed for the cassette design option with wings using the continuous energy Monte Carlo code MCNP-4A³. The nuclear data used is based on the FENDL-1 evaluation⁴. The detailed geometrical configuration of the divertor cassette has been modeled. The model represents a nine degree toroidal sector of ITER. The model includes in detail all cassette components. The 37.5 cm wide and 17.5 cm thick divertor pumping duct at the bottom of each cassette is included in the model. The rails upon which the cassettes move toroidally during maintenance are also included. Each divertor cassette in the model was divided into 103 regions to provide detailed spatial distribution of nuclear heating and radiation damage. The layered configurations of the dome PFC and vertical targets were modeled accurately. Separate regions are included in the model to represent the mechanical attachments and coolant pipe connections. Figure 3 shows a vertical cross section of the cassette model at the center of the cassette through the pumping ducts.

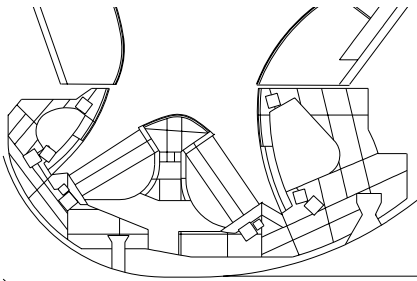


Fig. 3. Vertical cross section of the cassette model.

The divertor cassette model has been integrated with the general ITER model. The integrated model includes the first wall, blanket with associated coolant manifolds and back plates, VV, TF coils, central solenoid, and PF coils. While Be is used as the plasma facing material at the first wall, tungsten is used for the inboard and outboard baffle modules above the divertor cassette. All toroidal and poloidal gaps between adjacent blanket modules are

included. The major vacuum vessel penetrations are included in the model. The divertor port at the bottom of the reactor is 254.5 cm high with a width increasing from 97 cm at the bottom to 176 cm at the top. The port wall is 20 cm thick consisting of 80% 316SS and 20% water. The output of the MCNP geometry plotting routine given in Fig. 4 shows a vertical cross section through the middle of the VV ports. Figure 5 is a horizontal cross section at $z = -6$ m at the middle of the divertor port. The divertor pumping ducts in the divertor cassettes are shown in this figure. Also shown is the part of the TF coil adjacent to the divertor port. A coil case which is about 20 cm thick surrounds the winding pack. Several splitting surfaces have been added in the divertor region to allow for utilizing the geometry splitting with Russian Roulette variance reduction techniques³ needed to improve the accuracy of the calculated nuclear responses.

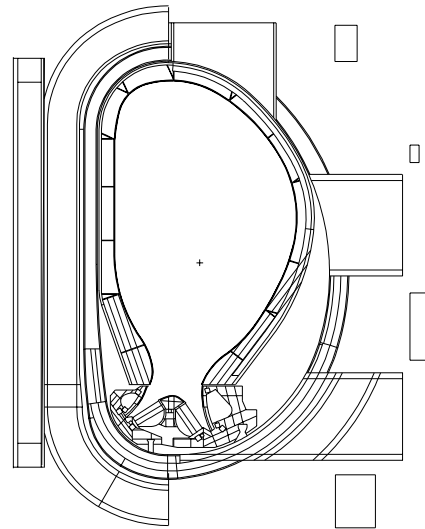


Fig. 4. Vertical cross section through the VV ports.

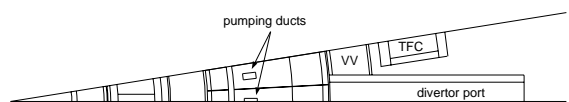


Fig. 5. Horizontal cross section at $Z = -6$ m.

The model employs 593 geometrical cells defined by 543 surfaces. Source neutrons are sampled from the source distribution in the ITER plasma provided numerically at 1600 mesh points. The VV consists of two 4 cm thick 316SS plates sandwiching a shielding region made of 60% 316SS and 40% water. The material composition used for the divertor cassette is given in

Table 1. The calculation has been performed using 50,000 source particles yielding statistical uncertainties less than 5% in the calculated nuclear responses at the locations of interest. The results are normalized to the nominal fusion power of 1500 MW. The end of life fluence related radiation effects have been determined for 1 full power year (FPY) of operation corresponding to a fluence of 1 MW.a/m².

Table 1. Material Composition in Divertor Cassette

Dome PFC	1 cm W 2 cm 75% Cu, 25% water Cu dome body 85% Cu, 15% water SS dome body 75% SS, 25% water
Wings	16% W, 79% Cu, 5% water packing fraction: 21% outer, 26% inner
Gas Box Liners	8% W, 74% Cu, 18% water
Vertical Targets	top section: 1 cm W 2.5 cm 82% Cu, 18% water back region 97% SS, 3% water lower section: 5.5 cm 89% C, 4% Cu, 7% water back region 97% SS, 3% water
Cassette Body	80% SS, 20% water
Mechanical Attachments	100% SS
Coolant Pipe Connections	70% SS, 30% water
Rails	100% SS

Geometrical configuration changes have been employed in the central part of the reference divertor cassette (Fig. 2). Only minor differences exist in the vertical targets and the inner and outer parts of the cassette body. The changes include an extended dome, elimination of the wings, and use of a thick dump target/liner in front of the pumping duct. In addition, the size of the pumping duct is different. Additional shielding is provided by the extended dome and the poloidally thicker central segment of the cassette body. The dump target and liner in the current design are combined into one component. The dump target, i.e. the lower part of the assembly has carbon fiber composite (CFC) as the PFC. In the upper and central parts of the assembly, 8 mm poloidal slots are incorporated to allow gas from the divertor channels to be exhausted into the pumping ducts. Chevron shaped W armor blocks are utilized as PFC in the liner.

The dome is coated with a 1 cm thick tungsten PFC as in the previous design. This is followed by a 2.2 cm thick Cu layer that includes 17% water coolant. The rest of the dome is made of SS with 15.3% water. The target/liner assembly is 12 cm thick and has six areas with three different compositions. The two slotted areas through which the gases flow into the pumping ducts consist of 9% W, 8% Cu, 28% SS, 6% water, and 49% void. The three transition areas representing the rest of the liner consist of 18% W, 18% Cu, 56% SS, and 8% water. The dump target has a front 4.5 cm layer made of CFC with 10% water and followed by a SS region with

5% water. The material compositions for the vertical targets, cassette body, mechanical attachments, and coolant pipe connects have not changed and are the same as those given in Table 1.

III. NEUTRON WALL LOADING DISTRIBUTION

The poloidal distribution of the neutron wall loading has been determined. In this calculation, only the uncollided neutron current crossing the front surface of the divertor cassette is tallied. Two million source particles have been sampled in the calculation yielding statistical uncertainty less than 0.5% in the calculated wall loading. Figure 6 gives the results in the divertor cassette design option with wings as a function of toroidal length measured in the counter-clockwise direction from the upper corner of the inner vertical target. The neutron wall loading peaks at 0.56 MW/m² in the dome which has the largest view of the plasma. The plasma view factor for the inner vertical target is very small resulting in very low neutron wall loading. The average neutron wall loading in the divertor cassette is 0.16 MW/m².

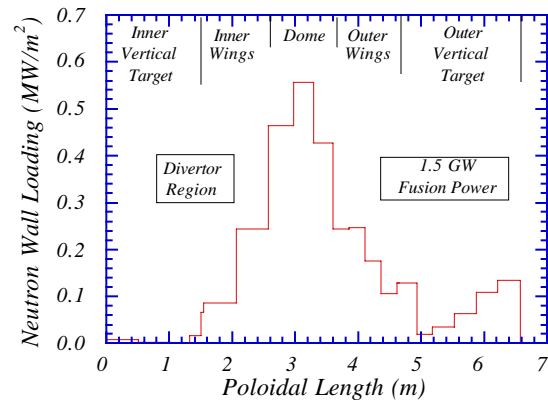


Fig. 6. Poloidal neutron wall loading distribution in the divertor cassette design with wings.

Figure 7 gives the poloidal variation of the neutron wall loading in the reference divertor cassette design shown in Fig. 2. The peak neutron wall loading in the dome does not change (0.56 MW/m²). The configurations of the inner and outer vertical targets in the new design result in the upper parts of them having a larger view of the plasma resulting in higher peak neutron wall loadings in them. The peak wall loading values in the inner and outer vertical targets are 0.08 and 0.17 MW/m², respectively. The sides of the dome and the vertical sections of the liners have a very restricted view of the plasma leading to significant dips in the neutron wall loading. The lower parts of the liners have higher wall loading values compared to the lower parts of the wings of

the previous design. The peak wall loading values in the inner and outer liners are 0.16 and 0.19 MW/m², respectively. The average neutron wall loading in the divertor cassette is 0.14 MW/m².

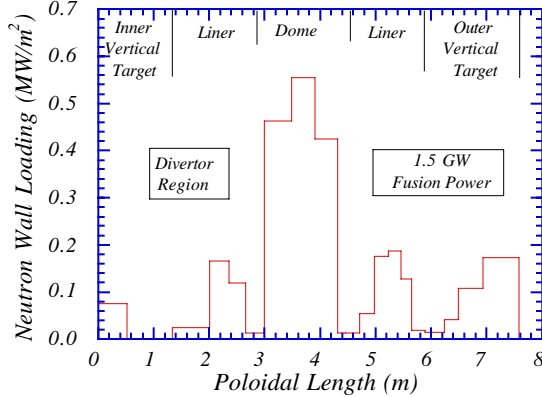


Fig. 7. Poloidal neutron wall loading distribution in the reference divertor cassette design.

IV. NUCLEAR PARAMETERS IN THE DIVERTOR CASSETTE

The nuclear parameters have been calculated in the different components of the divertor cassette. These included nuclear heating, atomic displacement and helium production. The volume averaged parameters were determined for 103 segments of the cassette. The largest heating and damage occurs in the dome PFC which has a full view of the plasma. The power density in the W PFC at the dome is 16.4 W/cm³. The W PFC at the top of the vertical targets experiences relatively high levels of heating and damage. The rest of the vertical targets and wings or liners experience moderate levels of heating and damage with values dropping rapidly as one moves deeper in the cassette body. In general, the nuclear parameters in the inboard side of the cassette are lower than in the outboard side which has a larger view of the plasma. Table 2 compares the peak nuclear parameters in the cassette components for the reference design and the previous design option with wings.

The peak nuclear heating and damage in the dome PFC of the reference design are similar to those in the previous design. The nuclear parameters decrease as one moves from the dome front surface deeper into the dome body. The pace of decrease is similar to that in the previous design for the front 30 cm of the dome. However, if one moves deeper into the dome beyond this distance, the nuclear parameters drop faster at the center of

the new extended dome design due to the added attenuation for the contribution from the sides of the dome. The coolant connections and mechanical attachments at the bottom of the dome are shielded from neutrons coming from the dome side by about 20 cm of the extended dome side and about 20 cm of the top solid region of the liner. This compares to a total shielding of only about 14 cm (40 cm wings at 20% density factor and 6 cm gas box liner) in the previous design. The additional shielding provided in the new design results in about a factor of 20 lower heating and damage.

The nuclear parameters in the dump targets at the bottoms of the inner and outer channels are slightly different from those for the previous design because of the different configurations of the vertical targets and the dump targets. The liners are exposed to direct source neutrons except for the top regions that are shielded by the extended dome. The lower regions of the liners experience peak nuclear parameters larger than those in the associated target dumps because of the increased view of the plasma. The nuclear parameters in the vertical regions of the liners decrease as one moves towards the dome due to added shielding by the extended dome. The configuration of the outer vertical target in the reference design results in the upper part of it having full view of the plasma and, consequently, higher nuclear parameters. The combined effect of increased poloidal thickness of the central part of the cassette and enhanced shielding by the extended dome yields nuclear parameters at the center of the cassette that are about a factor of 20 lower than in the previous design at elevations close to the dome with the reduction factor decreasing as one moves towards the bottom of the cassette.

The nuclear heating map in the previous cassette design option is given in Fig. 8. The total nuclear heating in the 60 divertor cassettes is 101.6 MW. In this design, the dome contributes about 31 MW of the total nuclear heating. The new dome increased in volume by about 25%. As a result, the contribution of the dome to total nuclear heating increases to about 40 MW. The total contribution from the new central body, dump target, and liner is 30 MW which is lower than the total contribution from the wings (29 MW), gas box liner (4 MW), and central body (5 MW) in the previous design. The reduced contribution is mainly due to additional shielding provided by the poloidally extended dome. The contribution from the rest of the cassette body and the vertical targets remains the same with the largest contribution being 23 MW from the vertical targets. The total nuclear heating in the cassettes is 102 MW which is similar to that for the previous design. Fig. 9 gives the nuclear heating map in the reference divertor cassette design.

Table 2
Peak Nuclear Responses in the Divertor Cassette Components

Zone	Power Density (W/cm ³)		dpa in Structure (dpa/FPY)		He Production in Structure (appm/FPY)	
	Reference Design	Previous Design	Reference Design	Previous Design	Reference Design	Previous Design
Dome PFC	16.4	16.4	1.3 W 3.5 Cu	1.3 W 3.5 Cu	0.7 W 31 Cu	0.7 W 31 Cu
Dome Body	3.8	3.9	1.9 Cu	2.1 Cu	16 Cu	17 Cu
Central Body	0.5	0.4	0.1 SS	0.1 SS	2.9 SS	2.5 SS
Outer Wings	NA	3.1	NA	1.7 Cu	NA	14 Cu
Inner Wings	NA	3.0	NA	1.6 Cu	NA	14 Cu
Outer Leg	0.6	0.5	0.12 SS	0.1 SS	3.9 SS	3.7 SS
Inner Leg	0.5	0.3	0.06 SS	0.04 SS	2.5 SS	2 SS
Outer Vertical Target	15	12	1.2 W 2.4 Cu 1.1 SS	0.9 W 1.9 Cu 0.8 SS	0.7 W 17 Cu 12 SS	0.5 W 13 Cu 9 SS
Inner Vertical Target	11	8.4	0.6 W 1.1 Cu 0.5 SS	0.4 W 0.8 Cu 0.3 SS	0.24 W 4.1 Cu 4.9 SS	0.07 W 1.9 Cu 3.1 SS
Outer Dump Target	1.3	1.5	0.5 Cu	0.64 Cu	4 Cu	5.1 Cu
Inner Dump Target	1	0.9	0.3 Cu	0.24 Cu	2 Cu	1.1 Cu
Outer Liner	2.1	0.8	0.9 Cu	0.3 Cu	9.6 Cu	1.6 Cu
Inner Liner	1.9	0.7	0.8 Cu	0.3 Cu	9.3 Cu	1.5 Cu
Rails	0.014	0.007	0.004 SS	0.002 SS	0.05 SS	0.03 SS

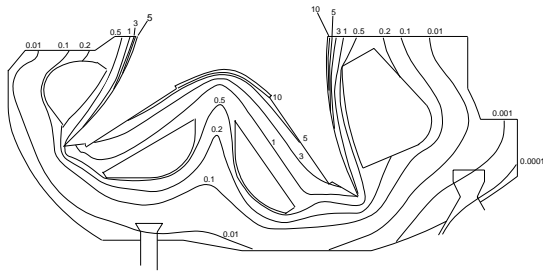


Fig. 8. Nuclear heating (W/cm³) map in the divertor cassette design option with wings.

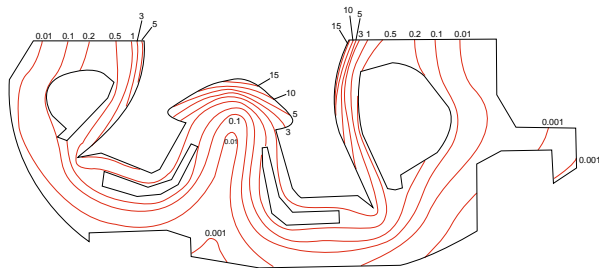


Fig. 9. Nuclear heating (W/cm³) map in the reference divertor cassette design.

V. NEUTRON STREAMING AND IMPACT ON VACUUM VESSEL

Pumping is achieved through a “Y” shaped pumping duct at the bottom of the cassette. This duct has a toroidal width of 17.5 cm. The duct outlet at the bottom of the cassette has a poloidal width of 45 cm in the reference cassette design compared to 37.5 cm in the previous design option. The VV behind the duct does not see any direct neutrons from the plasma which helps cut down the He production that is critical for rewelding. For rewelding to be feasible, the He production should be limited to 1 appm. The 3-D model was used to determine the VV nuclear responses for toroidal locations away from the ducts and behind the ducts. A peaking factor of about 2 results from streaming through the ducts in the previous cassette design. The peak helium production value of about 0.18 He appm/FPY indicates that rewelding parts of the VV behind the pumping ducts will be feasible.

In the reference cassette design, the 12 cm thick liner provides some attenuation for neutrons before streaming

into the duct. The effective shielding thickness at the duct opening is about 7 cm. The duct opening in the new reference design is about 40% larger than in the previous design option. An effective shielding thickness of 8 cm is provided in front of the duct by the wings in the previous design option. Therefore, about the same shielding effect is provided for the duct by the liner in the new design and the wings in the previous design. The main difference in VV damage is related to the 40% larger duct in the present reference design yielding a peak He production rate of 0.22 He appm/FPY in the VV. Rewelding parts of the VV behind the duct remains feasible.

Another area of concern for rewelding is the divertor port where relatively high damage is expected due to neutron streaming. The helium production was calculated along the divertor port. The largest damage occurs at the location where the port wall joins to the front VV wall. The peak helium production is 0.036 appm/FPY and drops to 0.005 appm/FPY at locations adjacent to the back of the TF coil. It is clear from these results that rewelding of the divertor port is feasible.

In an effort to optimize pumping, increasing the toroidal width of the gap between adjacent cassettes from the present 1 cm up to 4 cm is being considered. This increase takes place only in the lower region of the central part of the cassette body with the gap remaining at 1 cm for the rest of the cassette. A 3-D calculation was performed for the ITER-CDA design to determine the effect of assembly gap width between adjacent blanket and shield modules on peak VV damage⁵. For a blanket/shield thickness of 50 cm, the He production rate in the VV behind a 1 cm gap was a factor of 1.3 higher than without the gap. The peak values were factors of 2 and 5 higher than the case without the gap for gap widths of 2 and 4 cm, respectively.

As long as the gap width remains at 1 cm in the dome region and upper region of the central cassette body with a total depth of about 80 cm, no significant damage peaking in the VV behind the central region of the cassette is expected to result from increasing the gap width in the lower part of the cassette because of the shielding provided by the upper regions. The situation is different if large gaps are used in the cassette body below the lower parts of the liners. In this case, the 1 cm gap extends over a small depth determined by the liner thickness and the damage peaking is determined by the gap width in the cassette body with minimal additional shielding provided by the liner. If the gap in this region is increased to 4 cm, the peak VV damage behind it will be a factor of 5 higher than the case without the gap. This corresponds to about 0.5 He appm/FPY which still allows for rewelding.

VI. MAGNET RADIATION EFFECTS

The peak magnet radiation effects have been calculated in segments of the TF coils in the divertor region. No additional shielding is included around the port. In addition, no credit is taken for attenuation in coolant pipes, cryopumps, and other components in the port. The contribution from neutrons in the space between the outboard blanket back plate and the VV is overestimated since the 3 cm thick gas seal located above the divertor port between the VV and blanket was not included. The detailed calculations were performed using the divertor cassette design option with wings. However, since the configuration of the outer section of the cassette in front of the port opening did not change in the reference cassette design, the magnet damage results are relevant for the reference design. Table 3 gives the magnet radiation effects in the part of the TF coil adjacent to the divertor port. The radiation effects are higher at the side surface due to the effect of streaming through the port. The calculated radiation effects are much lower than the radiation limits considered in ITER⁶. It is clear that the sides of the TF coils are well protected from radiation streaming into the divertor ports.

Table 3. Magnet Radiation Effects at Front and Side Surfaces of the TF Coils Adjacent to the Divertor Port

	Front surface	Side surface	Design limit
Coil case power density (kW/m ³)	0.080	0.126	2
Winding pack power density (kW/m ³)	5.12x10 ⁻³	6.38x10 ⁻³	1
Insulator dose (Rad/FPY)	4.46x10 ⁶	6.78x10 ⁶	1x10 ⁹
Fast neutron fluence (n/cm ² per FPY)	6.27x10 ¹⁵	1.10x10 ¹⁶	1x10 ¹⁹
Copper dpa (dpa/FPY)	2.38x10 ⁻⁶	4.46x10 ⁻⁶	6x10 ⁻³

The total nuclear heating in the parts of the 20 TF coils in the divertor region is calculated to be 2.1 kW with 1.6 kW contributed by the parts adjacent to the divertor port. Subsequent calculations that included the inter-coil structures above and below the port indicated that the total heating in the TF coils and inter-coil structure around the divertor ports is 7.6 kW⁷. Dose rate calculations indicated that a 23 cm thick plate (75% SS and 25% water) is needed between the VV and blanket instead of the 3 cm thick gas seal in order to allow personnel access two weeks after shutdown in the area around the divertor port.

Including this shield in the calculations resulted in reducing nuclear heating in the TF coils and inter-coil structure in the divertor region to 0.5 kW⁷. The total nuclear heating in the TF coils should not exceed 17 kW. Adding the calculated nuclear heating for the different regions of the TF coils including streaming through all VV ports, the total nuclear heating is estimated to be about 7 kW⁷.

VII. SUMMARY AND CONCLUSIONS

The detailed geometrical configuration of the divertor cassette has been modeled for 3-D neutronics calculations. The layered configurations of the dome PFC and vertical targets were modeled accurately with the front tungsten layer modeled separately. The divertor cassette model was integrated with the general ITER model. The source neutrons were sampled from the source distribution in the ITER plasma. For the nominal 1500 MW fusion power, the peak neutron wall loading in the divertor region is 0.56 MW/m² at the divertor cassette dome which has full view of the plasma.

3-D neutronics calculations have been performed to determine the detailed spatial distribution of the nuclear parameters in the divertor cassette. These parameters included power density, atomic displacement and helium production. The largest heating and damage occurs in the dome PFC which has full view of the plasma. The power density in the tungsten PFC at the dome is 16.4 W/cm³. In general, the nuclear parameters in the inboard side of the cassette are lower than those in the outboard side which has a larger view of the plasma. The local nuclear parameters in the components of the reference cassette design are similar or lower than those in the cassette design option with wings. The total nuclear heating in the 60 divertor cassettes is 102 MW for both designs.

Radiation damage to parts of the vacuum vessel in the divertor region were quantified to assess the feasibility of rewelding. The peak helium production in the VV behind the pumping ducts is 0.22 He appm/FPY implying that rewelding is feasible. In addition, helium production in the divertor port wall is less than 0.04 He appm/FPY. Increasing the gap width between cassettes to 4 cm in the lower region of the cassette body below the dome and liners is acceptable with VV He production levels allowing for rewelding.

The impact of radiation streaming into the 20 large divertor ports on heating and damage in the TF coils was assessed. The port wall is 20 cm thick and is cooled by 20% water. The TF coils are well protected from radiation streaming into the divertor ports. The total nuclear

heating in the parts of the TF coils and inter-coil structure in the divertor region is only 0.5 kW when a 23 cm plate shield is used between the VV and blanket at the location of the gas seal above the divertor port.

ACKNOWLEDGMENTS

This report is an account of work performed under the Agreement among the European Atomic Energy Community, the Government of Japan, the Government of the Russian Federation, and the Government of the United States of America on Cooperation in the Engineering Design Activities for the International Thermonuclear Experimental Reactor ("ITER EDA Agreement") under the auspices of the International Atomic Energy Agency (IAEA).

REFERENCES

1. Technical Basis for the ITER Final Design Report, Cost Review and Safety Analysis, ITER EDA Documentation Series, International Atomic Energy Agency, Vienna, December 1997.
2. K. Dietz, T. Ando, A. Antipenkov, et al., "The ITER Divertor," Proc. IEEE 16th Symposium on Fusion Engineering, Champaign, IL, Sept. 30-Oct. 5, 1995, IEEE Cat. No. 95CH35852, Vol. 1, pp. 144.
3. J. Briesmeister, Ed., "MCNP, A General Monte Carlo N-Particle Transport Code, Version 4A," LA-12625-M (1993).
4. R. MacFarlane, "FENDL/MC-1.0, Library of Continuous Energy Cross Sections in ACE Format for MCNP-4A," Summary Documentation by A. Pashchenko, H. Wienke and S. Ganesan, Report IAEA-NDS-169, Rev. 3, International Atomic Energy Agency (Nov. 1995).
5. L. El-Guebaly and M. Sawan, "Shielding Analysis for ITER with Impact of Assembly Gaps and Design Inhomogeneities," Proc. 8th International Conf. on Radiation Shielding, Arlington, Texas, 24-28 April 1994, pp. 1047.
6. ITER General Design Requirements, International Thermonuclear Experimental Reactor, 22 March 1996.
7. R.T. Santoro, V. Khripunov, H. Iida, et al., "ITER Nuclear Analysis Report," ITER Nuclear Analysis Report No. NAG-100-12-01-97, Dec. 1997.